

A characteristic approach to the quasi-normal mode problem

Lars Samuelsson^{1*}, Nils Andersson^{1†} and Asimina Maniopoulou¹

¹ School of Mathematics, University of Southampton, Southampton SO17 1BJ, UK

Abstract

In this paper we discuss a new approach to the quasi-normal mode problem in general relativity. By combining a characteristic formulation of the perturbation equations with the integration of a suitable phase-function for a complex valued radial coordinate, we reformulate the standard outgoing-wave boundary condition as a zero Dirichlet condition. This has a number of important advantages over previous strategies. The characteristic formulation permits coordinate compactification, which means that we can impose the boundary condition at future null infinity. The phase function avoids oscillatory behaviour in the solution, and the use of a complex radial variable allows a clean distinction between out- and ingoing waves. We demonstrate that the method is easy to implement, and that it leads to high precision numerical results. Finally, we argue that the method should generalise to the important problem of rapidly rotating neutron star spacetimes.

1 Introduction

The dynamical oscillations of compact objects is a problem of great relevance for general relativistic astrophysics. Interesting questions range from observational to theoretical, with the possibility of detecting gravitational waves from pulsating neutron stars and black holes and using the signals to infer source parameters providing strong motivation for detailed studies. From the more theoretical point of view, the stability properties of these astrophysical bodies are intimately linked to their oscillation spectra. For rotating neutron stars, this is clearly demonstrated by the gravitational-wave driven instability that was first discussed by Chandrasekhar [1], Friedman and Schutz [2].

In general relativity, non-radial fluid oscillations radiate gravitational waves. Hence the oscillation mode problem is conceptually different from that in Newtonian gravity. In order to determine the pulsation modes one must impose an outgoing-wave boundary condition at infinity. It is well documented that this leads to technical difficulties if the quasi-normal modes are rapidly damped. The main reason for this is that on a spacelike hypersurface, as obtained by assuming that the perturbation quantities have a $\exp(i\omega t)$ time-dependence, the required solutions grow exponentially towards infinity. In order to impose an accurate outgoing-wave condition one must be able to filter out the exponentially decaying ingoing-wave component.

Various methods have been devised to handle this problem, see the review by Kokkotas and Schmidt [3] for an exhaustive discussion. One approach, that has the advantage that it is relatively easy to implement, is based on the use of analytic continuation and integration of the perturbation equations for complex values of the radial variable. The method, which was first used to calculate accurate quasi-normal modes of black

*E-mail: lars@soton.ac.uk

†E-mail: na@maths.soton.ac.uk

holes [4], has been successfully applied to the stellar oscillation problem [5].

The main outstanding problem in this area concerns the oscillations of rapidly spinning relativistic stars. In this case the perturbation equations that need to be solved in the exterior vacuum are no longer describable by a single wave-type equation (essentially because the spacetime is no longer of Petrov type D [6]). This makes the solution more involved and, in particular, any method that relies on the solution of a single separated differential equation no longer applies. This problem has yet to be overcome. The best results that we have correspond on the one hand to the so-called neutral modes [7, 8], identifying the points where the fundamental f-mode becomes susceptible to the Chandrasekhar-Friedman-Schutz instability, and on the other hand to modes determined after ignoring the metric perturbations (within the relativistic Cowling approximation) [9]. In the latter case one can use multipole formulae to estimate the damping/growth rate of the modes. Nevertheless, the situation is not satisfactory. After all, it is not clear how accurate the Cowling approximation will be for the various classes of modes that one may be interested in. There is a clear need for a more detailed solution to the mode-problem for rapidly rotating neutron stars.

This paper introduces a new strategy to the problem. The main idea is to use a characteristic formulation of the perturbation problem [10] to avoid the diverging eigenfunctions that plague the standard analysis. By considering two simple model problems, we will demonstrate the promise of this approach. Most importantly, we will show how one can formulate the outgoing-wave condition as a Dirichlet condition for a suitably introduced phase-function [11]. Taken together with the fact that a characteristic formulation permits coordinate compactification without the loss of resolution [12], this enables us to impose the desired boundary condition at future null infinity with extreme precision. We illustrate the key features of the new method by applying it to the well-studied problem of axial spacetime modes of a uniform density star. Using a spectral approach to solve for the relevant phase-function in the exterior of the star, we obtain results with very high numerical precision. The reliability of the method is shown by considering an ultra-compact star, with $R/M = 2.26$, which has both very slowly and very rapidly damped modes. We confirm previous results for the slowly damped modes, and even provide some new results by identifying several previously unknown interface w -modes. This result is likely irrelevant from the astrophysics point of view, but it is conceptually interesting since it hints at the possibility that there may exist an infinite number of such modes.

The numerical results that we report are in themselves not particularly interesting. The main achievement is the successful new formulation of the quasi-normal mode problem that should be straightforward to extend to the rapid rotation case. The characteristic formulation of the Einstein equations is of course well-known, and we cannot see any real difficulties in generalising our method to the resultant coupled perturbation equations. In fact, the possibility of having a Dirichlet condition at infinity in the computationally more involved two-dimensional problem is very attractive. Some details obviously remain to be worked out. The main issue concerns phase-functions for coupled equations, a problem that has already been considered in quantum scattering problems [13]. Hence, we feel very optimistic. For the first time we have a truly promising strategy for dealing with one of the most challenging problems in this area of research, the determination of oscillation modes and the associated gravitational-wave damping/growth rate for fast spinning stars.

1.1 Problem setup

As a model problem we will consider the mode problem in static spherically symmetric spacetimes. In particular, the wave equations we will discuss in this paper can all be written on the form

$$(\mathcal{D}_a \mathcal{D}^a - U)\psi = 0 \quad (1)$$

where \mathcal{D}_a is the covariant derivative on the submanifold orthogonal to the spherical symmetry surfaces (a runs from 0 to 1) and U is an effective potential depending only on the radial coordinate. For vacuum perturbations the potential is of the form

$$U = \frac{l(l+1)}{r^2} - \frac{6M}{r^3} \mathcal{U}_\pm \quad (2)$$

where

$$\mathcal{U}_- = 1 \quad (3)$$

$$\mathcal{U}_+ = \frac{[l^2(l+1)^2 - 4]r^2 + 12M(r - M)}{[(l-1)(l+2)r + 6M]^2} \quad (4)$$

for axial and polar perturbations, respectively. Here M is the mass, r is the Schwarzschild radial coordinate and $l \geq 2$ is the usual angular “quantum number” originating from the separation of the angular dependence. Asymptotically the polar piece approaches a constant;

$$\mathcal{U}_+ \sim \frac{l(l+1) + 2}{l(l+1) - 2} \quad (5)$$

and it is easy to show that $\frac{5}{7} \leq \mathcal{U}_+ \leq 2$ everywhere outside $r = 2M$. It is evident that the asymptotic behaviour of the axial and polar perturbations is very similar. For this reason we restrict our attention, from now on, to the axial sector.

We shall later, as a test case, consider axial perturbations of perfect fluid stars. These are also governed by an equations of the form (1), with U given by

$$U = \frac{l(l+1)}{r^2} - \frac{6m}{r^3} + \frac{\kappa}{2}(\rho - p) \quad (6)$$

where $m = m(r)$ is the mass inside r , ρ is the energy density and p is the pressure [14, 15].

In our analysis of the wave equation (1) we shall use our freedom of choice of coordinates. It is conventional to adapt the coordinates to the timelike Killing vector on the background and choose the remaining radial coordinate to be either the Schwarzschild area radial function r or the Regge-Wheeler tortoise radius r_* . The former has the advantage of being invariantly defined as giving the area of a spherical symmetry surface through $\text{Area} = 4\pi r^2$. On the other hand, the tortoise coordinate is intimately related to the characteristics of the wave equation for massless fields and is related to r (in vacuum) through

$$r_* = r + 2M \ln[C(r - 2M)] \quad (7)$$

where C is a constant related to translations. Since we are primarily interested in the asymptotics (which does not depend strongly on whether r or r_* is used) we shall use r in the following.

An alternative to using the Killing time as a coordinate is to use *characteristic* coordinates as introduced by Bondi *et al.*[16] and Sachs [17]. The relation between the different coordinates is

$$x = r \quad (8)$$

$$u = t - r_*(r) \quad (9)$$

where u is the retarded time and the characteristic radial variable x is actually the same as the area radius and we shall soon denote it by r . However it is important to remember that

$$\frac{\partial}{\partial r} = \frac{\partial x}{\partial r} \frac{\partial}{\partial x} + \frac{\partial u}{\partial r} \frac{\partial}{\partial u} = \frac{\partial}{\partial x} - \frac{dr_*}{dr} \frac{\partial}{\partial u} \quad (10)$$

For vacuum spacetimes and for the coordinates discussed above the line elements can be written

$$ds^2 = ds_j^2 + r^2(d\theta^2 + \sin^2\theta d\phi^2) \quad (11)$$

where

$$ds_j^2 = -e^{2\nu} du^2 - 2du dr \quad \text{Bondi-Sachs (B)} \quad (12)$$

$$ds_j^2 = -e^{2\nu} dt^2 + e^{-2\nu} dr^2 \quad \text{Schwarzschild (S)} \quad (13)$$

We have set $x = r$ and introduced the notation

$$e^{2\nu} = 1 - \frac{2M}{r} \quad (14)$$

The wave equation (1) can now be explicitly written down

$$-2\psi_{,ur} + e^{2\nu}\psi_{,rr} + \frac{2M}{r^2}\psi_{,r} - U\psi = 0 \quad (\text{B}) \quad (15)$$

$$-e^{-2\nu}\psi_{,tt} + e^{2\nu}\psi_{,rr} + \frac{2M}{r^2}\psi_{,r} - U\psi = 0 \quad (\text{S}) \quad (16)$$

Note that, in the characteristic formulation, there is no second derivative with respect to the “time” u . To find mode solutions we take the time dependence to be given by $\psi \propto e^{i\omega T}$ where $T = t, u$ depending on coordinates. We let primes denote derivatives with respect to the spatial coordinate (remember that the primes are different due to (10)!).

$$e^{2\nu}\psi'' + 2\left(\frac{M}{r^2} - i\omega\right)\psi' - U\psi = 0 \quad (\text{B}) \quad (17)$$

$$e^{2\nu}\psi'' + \frac{2M}{r^2}\psi' - (U - e^{-2\nu}\omega^2)\psi = 0 \quad (\text{S}) \quad (18)$$

We may note here that the algebraic transformation $\psi \rightarrow e^{-i\omega r_*}\psi$ brings the Schwarzschild equation to the form of the Bondi-Sachs equation. Thus for the simple case of static spacetimes considered here we can mimic the characteristic approach by this simple transformation. However, the case we are really interested in is the two-dimensional rapidly rotating problem where such a trick is not likely to exist.

2 A pedagogical toy problem

Since the main interest in this paper is the behaviour of wave solutions in the asymptotically flat region of spacetime far away from the source we will begin by considering the very illustrative toy problem in which M is set to zero. It should be intuitively clear, and it will later be demonstrated, that this problem has the same properties near infinity as the $M \neq 0$ case. A great advantage is that it allows for an exact solution. In fact, in Schwarzschild coordinates

$$\psi = \sqrt{r}[C_{\text{in}}H_{l+1/2}^{(1)}(\omega r) + C_{\text{out}}H_{l+1/2}^{(2)}(\omega r)] \quad (\text{S}) \quad (19)$$

where $H^{(1)}$ and $H^{(2)}$ represent the in- and outgoing Hankel (or Bessel of the third kind) functions and the constants refer to the proportion of out- and ingoing waves as can be seen from the asymptotic behaviour

$$\psi e^{i\omega t} \sim C'_{\text{in}}e^{i\omega(t+r)} + C'_{\text{out}}e^{i\omega(t-r)} \quad (\text{S}) \quad (20)$$

As noted previously, in Bondi-Sachs coordinates the solution is just given by multiplying the Schwarzschild solution by $e^{i\omega r_*} = e^{i\omega r}$. In order to illustrate the nature of these solutions we will now examine the special case of $l = 2$. Then the solution becomes, after some redefinitions of the constants,

$$\psi = C_{\text{in}}\frac{\omega^2 r^2 + 3i\omega r - 3}{\omega^2 r^2}e^{i\omega r} - C_{\text{out}}\frac{\omega^2 r^2 - 3i\omega r - 3}{\omega^2 r^2}e^{-i\omega r} \quad (\text{S}) \quad (21)$$

For definiteness we will plot the solutions for an arbitrarily chosen frequency $\omega = 1 + i/10$ in units such that the inner boundary is located at $r = 1$. The ingoing and outgoing parts of the solution in Schwarzschild coordinates are plotted in figures 1a and 1b, respectively. If we imagine finding these solutions numerically we immediately note two problems. First the solutions are oscillating. This is clearly a problem since we are really interested in imposing boundary conditions at infinity and hence would like to compactify spacetime in order to cover it on a finite grid. It is evident, regardless of the number of grid points, that

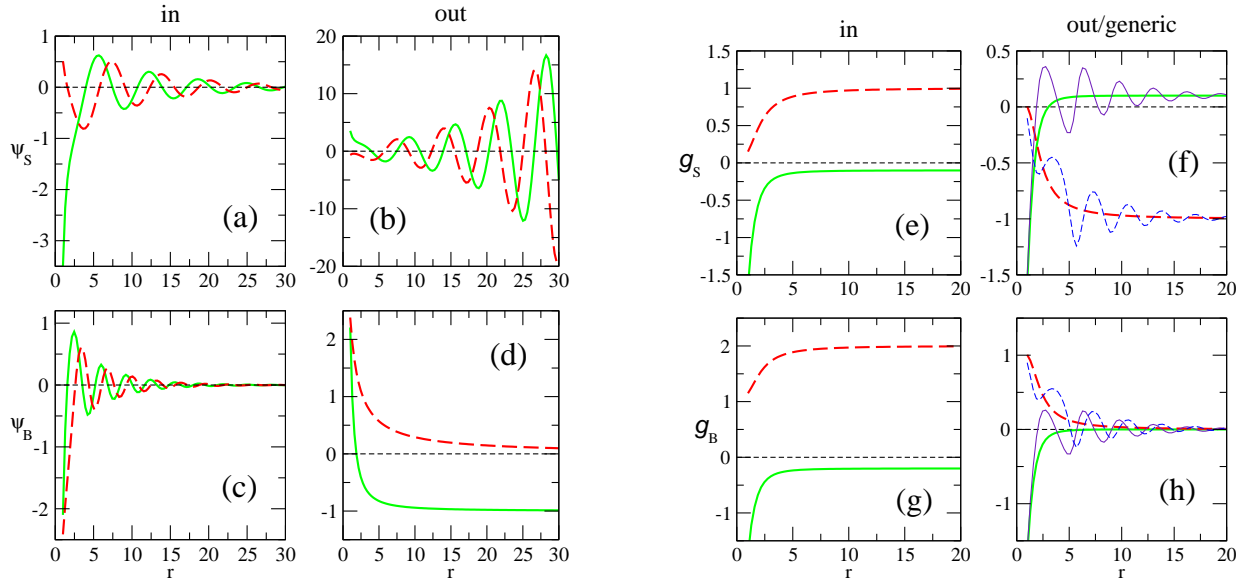


Figure 1: The left set of panels (a-d) display the real (solid) and imaginary (dashed) parts of the wave function ψ as a function of r . The right set (e-h) shows the phase function $g(r)$. In each set of four panels the top two (a-b and e-f) show the solution in Schwarzschild coordinates whereas the bottom two (c-d, g-h) display the characteristic solutions. The left panels (a,c and e,g) show the ingoing solutions while the right panels (b,d and f,h) instead display the outgoing solution. In panels f and h we additionally plot a generic solution with $C_{\text{in}} = 0.57$, $C_{\text{out}} = 1.3$. See the main text for further discussion.

the oscillating behaviour will not be resolved at some finite radius. The other problem is that the ingoing solution is exponentially decreasing outwards. Hence, it will be numerically impossible to distinguish the outgoing solution from a solution contaminated by an ingoing piece. In figures 1c and 1d we instead plot the characteristic/Bondi-Sachs form. The outgoing solution is clearly much better behaved here and would in principle be possible to track numerically on a compactified grid. However, the problem with the rapid decay of the ingoing solution remains.

The oscillation problem is often resolved by introducing a phase function. Several options exist which are essentially equivalent, see *e.g.* [11]. Here we simply define the phase function to be

$$g = \frac{\psi'}{\psi} \quad (22)$$

as suggested from WKB-type arguments. In figure 1e-h we show the behaviour of the phase function. Panels 1e and 1f show the ingoing and outgoing solutions in Schwarzschild coordinates whereas 1g and 1h are the Bondi-Sachs forms. In panels 1f and 1h we additionally show a generic solution with coefficients arbitrarily chosen to be $C_{\text{in}} = 0.57$ and $C_{\text{out}} = 1.3$. We see that although the phase function solves the problem of oscillating solutions we still cannot distinguish the outgoing solution from a generic one at infinity. The reason is that the transformation to the variable g is non-linear and pieces coming from the ingoing solution will always be exponentially suppressed for positive imaginary parts of ω . It is clear that we must find a way to remove the exponential decay of the ingoing solution in order to find a successful numerical scheme. Before turning to this problem it is useful to note that although all solutions are asymptotically constant, the outgoing Bondi-Sachs version has the advantage of being asymptotic to zero. Hence, in that formulation, the outgoing wave boundary condition can be replaced by a much simpler zero Dirichlet condition.

We turn now to the decay of the ingoing solution. The problem comes from the asymptotic factor

$$e^{i\omega r} = e^{i\Re(\omega)r} e^{-\Im(\omega)r} \quad (23)$$

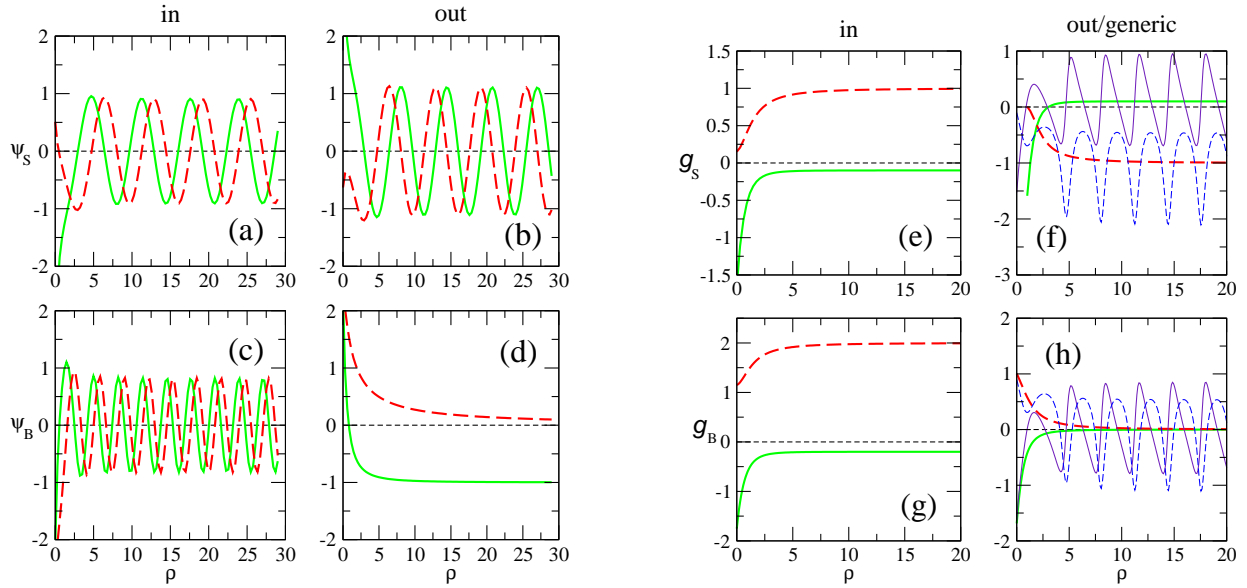


Figure 2: Same as figure 1 but with ϱ as radial coordinate. Hence, these solutions are obtained from integration in the complex r -plane.

There is a neat trick to resolve this problem which has been used for quasi-normal modes, see *e.g.* [4, 5]. The idea is to analytically continue the support of the dependent variable g or ψ and let the radial coordinate take on complex values. In this spirit we write

$$r = R + \varrho e^{i\vartheta} \quad (24)$$

where R is the (real) radius outside which we are interested in the solution and ϱ and ϑ are real. We now wish to choose the angle ϑ in the complex plane such that the decay of the ingoing solution is avoided. Substituting (24) into (23) we see that we must choose

$$\vartheta = -\arg(\omega) \quad (25)$$

Having made this choice¹ we plot the various solutions again in figure 2. Note that all divergent/decaying behaviour is gone. We see that, in principle, there exist three possibilities to implement a successful numerical scheme. The characteristic approach aided by the complex radial coordinate as displayed in panels 2c-d allows distinction of the in- and outgoing solutions together with compactification and imposition of boundary conditions at or near infinity. The same applies to the phase function approaches as shown in figures 2e-f (Schwarzschild) and 2g-h (Bondi-Sachs). However, the Bondi-Sachs phase function has the advantage of going asymptotically to zero. Hence, in this approach, the outgoing-wave boundary condition may be replaced by a zero Dirichlet condition on the phase function at null infinity. This is of course a great simplification when extensions to more general circumstances (such as rapidly rotating sources) are considered.

2.1 A numerical example

In order to show that the approach can be accurately implemented we now solve a toy quasi-normal mode problem. As above we take $M = 0$, and choose units in which $R = 1$. To complete the problem we choose boundary conditions such that, in Bondi-Sachs coordinates

$$\psi'|_{r=R} = g|_{r=R} = 0 \quad (26)$$

¹Obviously, $\omega = 0$ is a degenerate case in this respect and cannot be treated with the present approach. However, since the $\omega = 0$ problem for rotating stars has already been studied in detail by Stergioulas and coworkers [7, 8] this is not a serious drawback of our method.

l	Frequencies, exact	numerical
2	$2i$	$0.000000000 + 2.000000000i$
3	$\frac{1}{2}(\sqrt{5} + 5i)$	$1.118033989 + 2.500000000i$
7	$5.071731535 + 3.511061460i$	$5.071731535 + 3.511061460i$
	$2.947010505 + 4.736313493i$	$2.947 + 4.74i$
	$0.9710593605 + 5.252625048i$	$0.97106 + 5.2526i$

Table 1: Quasi-normal modes of the toy problem for various l . All the digits shown have converged and agree with the exact solution. In some cases we reach machine precision, see table 2. Note, however, the poor convergence for some of the $l = 7$ modes. See the main text for an explanation of this.

whereas, as shown above, g satisfies a zero Dirichlet condition at infinity. The inner boundary condition is chosen purely for mathematical convenience. In order to be able to enforce the boundary conditions at infinity we compactify spacetime by introducing the radial coordinate x through

$$x = \frac{r_1 - \varrho}{r_1 + \varrho} \quad (27)$$

where the real constant r_1 makes it easier to keep track of the dimensions. Note that

$$r = R \quad \leftrightarrow \quad \varrho = 0 \quad \leftrightarrow \quad x = 1 \quad (28)$$

$$r = \infty \quad \leftrightarrow \quad \varrho = \infty \quad \leftrightarrow \quad x = -1 \quad (29)$$

so that the exterior spacetime is mapped to the domain $-1 < x \leq 1$. The reason we chose this range is that we base our numerical code on a Chebychev pseudo-spectral method, *e.g.* [18]. Using equations (15) and (22) we find that the phase function has to satisfy

$$g_{,x} = \frac{2r_2}{(x+1)^2}g^2 - \frac{4i\omega r_2}{(x+1)^2}g - \frac{2r_2l(l+1)}{[R(1+x) + r_2(1-x)]^2} \quad (30)$$

where $r_2 = r_1 e^{i\vartheta}$. As will be seen in the next section, the irregular singular point at infinity ($x = -1$) does not pose a problem for the outgoing solution since $g \sim (1+x)^2$ in the neighbourhood of null infinity. The purely ingoing solution is (of course) also well behaved since it asymptotically cancels the two first terms on the right hand side of (30). When we enforce the boundary conditions at infinity we add the point $x = -1$ and put $g = 0$ exactly there. This is one of the advantages of the pseudo-spectral approach – we are actually able to enforce the boundary conditions *at* infinity. The family of solutions to (30) then provide a function $g_s(\omega) = g(x=1, \omega)$ whose zeros correspond to the quasi-normal modes. At a practical level, we solve equation (30) by a Chebychev pseudo-spectral code using a Newton-Kantorovich scheme to turn the problem from a non-linear equation to iteratively solved linear equations (see *e.g.* the book by Boyd [18] for details on spectral methods). We iterate until the corrections to the solution are everywhere less than 10^{-15} . We solve the equation for a large set of frequencies. A contour plot of the absolute value of $g_s(\omega)$ is then used to locate the points in the complex frequency plane where $g_s(\omega)$ is close to zero. These points are then used as initial guesses in a Müller type root finder. We decided to use a spectral code since we expect this approach to generalise to the coupled partial differential equations which need to be solved in the rapidly rotating case.

We examine the cases $l \in \{2, 3, 7\}$. The eigenmodes in the positive quadrant are given in table 1. For the case $l = 2$ we see that we have the extreme case of a “mode” with purely imaginary frequency. In

N	Frequency	$2 - \omega $	$\frac{1}{2}\pi - \arg(\omega)$
40	$5.444541 \times 10^{-3} + 1.997613i$	-2.379953×10^{-3}	-2.725517×10^{-3}
80	$4.063484 \times 10^{-7} + 2.000000i$	4.089420×10^{-8}	-2.031742×10^{-7}
120	$1.893739 \times 10^{-11} + 2.000000i$	$-1.279776 \times 10^{-11}$	$-9.468648 \times 10^{-12}$
160	$3.011046 \times 10^{-15} + 2.000000i$	1.332268×10^{-15}	$-1.554312 \times 10^{-15}$
200	$-4.551599 \times 10^{-16} + 2.000000i$	4.440892×10^{-16}	2.220446×10^{-16}
240	$9.935105 \times 10^{-16} + 2.000000i$	$-6.661338 \times 10^{-16}$	$-4.440892 \times 10^{-16}$

Table 2: Convergence test for the $l = 2$ quasi-normal mode of the toy problem. The two right-hand columns show the error in the numerically obtained absolute value and phase of the frequency as compared with the exact value $\omega = 2i$. Machine precision is reached exponentially fast as the resolution (N) is increased.

table 2 we show the convergence of the solution as a function of grid points N . As we can see machine precision (in this case double $\sim 10^{-16}$) is reached exponentially fast, a trade mark of a spectral code. The convergence is equally impressive for $l = 3$. For the case $l = 7$, however, we run into problems. The first mode ($\omega \approx 5.07 + 3.51i$) is found without problems, but as the argument of the frequency starts growing the code runs into convergence problems. The reason for this behaviour can be seen from the exact solution. For any $l \geq 2$ the solutions have the general form (in terms of r)

$$g = \frac{\sum_{i=0}^{l-1} a_i(l)(\omega r)^i}{r \sum_{i=0}^l b_i(l)(\omega r)^i} \quad (31)$$

where $a_i(l)$ and $b_i(l)$ are constants depending on l . As we can see, these functions have a number of poles determined by the zeros of the polynomial in the denominator. If any of these poles happen to lie close to our path of integration we can expect large variations in g . This is indeed what happens for $l = 7$, causing convergence problems for the spectral code (which relies crucially on the smoothness of the solution). We have tried to use other integration routines and found it straightforward to improve the accuracy of the obtained frequencies. However, the main goal here is not to obtain accuracy in this highly unphysical toy problem, but rather to assess the pros and cons of our proposed characteristic scheme. Hence, the convergence problems displayed in table 1 only serve as a nice reminder of the kind of problems that can be encountered in real situations. We should note here that if a pole should happen to lie exactly in the path of integration the method presented here will fail. This seems highly unlikely to happen however and is not related to the characteristic approach, but rather to the analytic continuation and introduction of a complex r .

3 Quasi-normal modes of uniform density “stars”.

We now turn to the slightly more relevant problem of finding the axial w -modes of a constant density star. This problem has been treated many times before (*e.g.* [19, 15, 20, 21]) allowing us to compare our results to the existing ones. Since the behaviour near null infinity is most strongly dependent on the frequency and not on the particulars of the wave function(s) near or in the star we believe that this comparatively simple problem serves as a sufficient test of our method as far as non-rotating stars are concerned. In order to span as large a region of frequency space as possible we concentrate on an ultra compact model for which $R = 2.26M$, *i.e.* quite close to the Buchdahl limit $R = 2.25M$. The w -mode spectrum [22] can then be

loosely divided into three parts (see [3]). The *trapped modes* [19] are characterised by a low damping rate, *i.e.* a small imaginary part of the frequency. These modes exist due to a peak in the potential near $r = 3M$ and correspond, in a loose sense, to almost bound states of the Schrödinger-like wave equation. For higher “energies” the modes become less and less bound (*i.e.* more damped), having increasingly large imaginary parts of the frequencies. These are the ordinary, or curvature, w -modes. An infinite number of these modes is likely to exist.

There also exist another branch of modes, the *interface*, or w_{II} -modes [23]. These are thought to correspond to scattering of gravitational waves off the “surface” of the star much like hard-sphere scattering of sound waves. These rapidly damped modes have large imaginary parts of the frequency. Previous numerical surveys have only found a few (typically two or three) such modes. With our method we are able to probe larger imaginary parts and discover many more w_{II} -modes, thus raising the question whether these modes also form an infinite family.

We now proceed to show that the analysis carried out in the preceding section generalises to spherically symmetric spacetimes with arbitrary M . We shall only consider the characteristic approach here. It is straightforward to show that the wave function has the asymptotic behaviour

$$\psi_{\text{out}} \sim 1 - \frac{il(l+1)}{2\omega r} + \frac{12iM\omega + 2l(l+1) + l^2(l+1)^2}{8\omega^2 r^2} + \dots \quad (32)$$

$$\psi_{\text{in}} \sim e^{2i\omega r} r^{4iM\omega} \left(1 - \frac{i[16M^2\omega^2 - l(l+1)]}{2\omega r} + \dots \right) \quad (33)$$

Using the relation (7) we can write

$$e^{2i\omega r} r^{4iM\omega} = e^{2i\omega r_*} \left[\frac{r}{C(r-2M)} \right]^{4iM\omega} \sim \frac{e^{2i\omega r_*}}{C^{4iM\omega}} \left[1 + \frac{8iM^2\omega}{r} + \dots \right] \quad (34)$$

The outgoing solution approaches a constant whereas the ingoing solution, which is proportional to $e^{2i\omega r_*}$, decays exponentially for damped modes. The phase function has the leading order behaviour

$$g = \frac{\psi'}{\psi} \sim \frac{\frac{il(l+1)}{2\omega r^2} C_{\text{out}} + 2i\omega e^{2i\omega r_*} C_{\text{in}}}{C_{\text{out}} + e^{2i\omega r_*} C_{\text{in}}} \quad (35)$$

so that, for damped modes,

$$g \sim g_{\text{out}} \sim \frac{il(l+1)}{2\omega r^2} \quad (36)$$

making manifest the problem of separating a general solution from a purely outgoing one. Introducing the complex r coordinate given in equation (24) we turn the damping exponentials into simple trigonometric functions so that for large ϱ and $C_{\text{in}} \neq 0$

$$g \sim \frac{2i\omega e^{2i|\omega|\varrho} C_{\text{in}}}{C_{\text{out}} + e^{2i|\omega|\varrho} C_{\text{in}}} \quad (37)$$

For $C_{\text{in}} = 0$, *i.e.* the outgoing solution, we have instead

$$g \sim \frac{il(l+1)\omega}{2|\omega|^2 \varrho^2} \rightarrow 0 \quad (38)$$

It is clear that if the boundary condition $g = 0$ is imposed “exactly at infinity”, there is no contamination of the unwanted solution whatsoever. However, one may ask whether this preferred state of affairs prevails if one is forced to impose the boundary conditions at some large but finite radius ϱ . Putting the expansions equal we find that the asymptotic condition for an outgoing solution to coincide with a generic solution at some given radial coordinate $\varrho = \varrho_\infty$ (say) is

$$e^{2i|\omega|\varrho_\infty} C_{\text{in}} \sim \frac{l(l+1)}{4|\omega|^2 \varrho_\infty^2} C_{\text{out}} \quad (39)$$

We see that for any finite ϱ_∞ there exist complex C_{in} and C_{out} such that numerical confusion between the wanted $C_{\text{in}} = 0$ solution and a mixed in- and outgoing solution arise². However, it is also clear that this solution has $C_{\text{in}} \sim (|\omega|\varrho_\infty)^{-2}C_{\text{out}}$ and is therefore very close to the wanted solution. Thus, the only situation where this can cause worries is when the ingoing solution is rapidly decaying as a function of radius in some region (so that when integrating from large radii this solution blows up). Such a blow up will indeed happen in black hole spacetimes and one should also be careful if stars more compact than $R \lesssim 3M$ are considered (due to the peak in the effective potential).

3.1 Numerical implementation

Performing the compactification as described in the previous section, *i.e.* changing the radial coordinate to

$$x = -\frac{r - R - r_2}{r - R + r_2} \quad \Leftrightarrow \quad r = R + r_2 \frac{1 - x}{1 + x} \quad (40)$$

and using the phase function (22) we obtain the equation

$$g_{,x} = \frac{2r_2}{(x+1)^2}g^2 + e^{-2\nu} \frac{4r_2}{(x+1)^2} \left(\frac{M}{r^2} - i\omega \right) g + e^{-2\nu} \frac{2r_2}{(x+1)^2} \left(\frac{6M}{r^3} - \frac{l(l+1)}{r^2} \right) \quad (41)$$

for the exterior vacuum perturbations. This equation is solved by the same routine that was applied to the toy problem of the previous section, supplying a function $g_s^E(\omega) = g(x=1, \omega)$. The interior is governed by the wave equation (15) with the potential given by (6). Since our main aim here is to demonstrate the usefulness of the approach to the exterior perturbations we used a very simple code for the interior problem. The equations were taken from [24] and are listed in the appendix. We integrated the wave function in Schwarzschild coordinates using an off the shelf Runge-Kutta routine. At the surface of the star the phase function was evaluated, remembering eq. (10) thus giving rise to the function $g_s^I(\omega) = g(r=R, \omega)$. Now $g_s^E(\omega)$ and $g_s^I(\omega)$ are guaranteed for every ω to satisfy the boundary conditions at infinity and $r=0$ respectively. It follows that the quasi-normal mode frequencies are determined by the continuity of g at the surface of the star, and are hence given by the roots of

$$g_s^{\text{tot}} = g_s^E(\omega) - g_s^I(\omega) = 0 \quad (42)$$

We used the same strategy to find the modes as in the toy problem. In figure 3 we display contour plots of $|g_s^{\text{tot}}|$. The modes appear as “islands” in this plot and using the locations of these islands as initial guesses for our Müller root finder we obtain the roots (*i.e.* the quasi-normal mode frequencies). A sample of the obtained frequencies are given in table 3. They are shown in figure 3 as black squares. All results agree well with those of Kokkotas [15, 25] and exactly with those of Tominaga, Saijo and Maeda [21]. In the left panel of figure 3 we show the interface modes. We have managed to locate eight such modes. This raises the question if these modes constitute an infinite family. For the most rapidly damped modes in this class we encounter convergence problems both in the interior and the exterior routines. The exterior problem is, however, less severe than the interior one and a relative accuracy of about one part in 10^9 in the eigenfunction is achieved with moderate resolution. The interior solution is more difficult to determine accurately. A quick glance at the eigenfunctions reveal why, they are rapidly oscillating and exponentially growing suggesting that a phase function approach would be beneficial also for the interior problem. As stressed above, we are mainly concerned with the methods here and did not consider it relevant to try to improve the accuracy of the interior solutions for this paper. From a theoretical point of view it would, however, be interesting to settle the question on the number of interface modes. In the right panel of figure 3 we display the trapped and curvature modes. For these modes we do not have any convergence problems.

²By this we do not mean that there is necessarily an exact coincidence of a mixed in/outgoing solution and the purely outgoing solution, only that two such solutions are numerically indistinguishable.

	$\Re(\tilde{\omega})$	$\Im(\tilde{\omega})$		$\Re(\tilde{\omega})$	$\Im(\tilde{\omega})$
\dagger	2.138639×10^{-1}	2.432061×10^{-9}		1.271223	4.583803×10^{-2}
\dagger	2.910115×10^{-1}	7.747252×10^{-8}		1.352193	4.963654×10^{-2}
\dagger	3.679986×10^{-1}	1.072543×10^{-6}		1.434156	5.297615×10^{-2}
\dagger	4.446349×10^{-1}	9.518605×10^{-6}		1.516856	5.584165×10^{-2}
\dagger	5.206390×10^{-1}	6.339316×10^{-5}		1.600034	5.824413×10^{-2}
	5.955793×10^{-1}	3.380602×10^{-4}	\ddagger	1.451160	5.401143×10^{-1}
	6.689607×10^{-1}	1.432267×10^{-3}	\ddagger	1.73434	1.39451
	7.409095×10^{-1}	4.508010×10^{-3}	\ddagger	2.01107	2.29027
	8.128027×10^{-1}	1.013574×10^{-2}	\ddagger	2.29394	3.19756
	8.859040×10^{-1}	1.725926×10^{-2}	\ddagger	2.5798	4.1068
	9.603731×10^{-1}	2.448020×10^{-2}	\ddagger	2.866	5.016
	1.036081	3.102749×10^{-2}	\ddagger	3.153	5.924
	1.113082	3.668522×10^{-2}	\ddagger	3.448	6.846
	1.191470	4.155932×10^{-2}			

Table 3: Dimensionless frequencies $\tilde{\omega} = \omega\sqrt{R^3/3M}$ of the axial $l = 2$ modes in a $R = 2.26M$ constant density star. The trapped modes, defined to be those whose frequency satisfy $\Re(\omega)^2 < V_{\max}$, are marked with a \dagger . Here $V_{\max} \approx 0.1513/M^2$ is defined to be the value of the effective potential in the Regge-Wheeler equation at the peak. The interface modes are marked by \ddagger . All digits shown should be correct and in many cases the accuracy is much better than displayed.

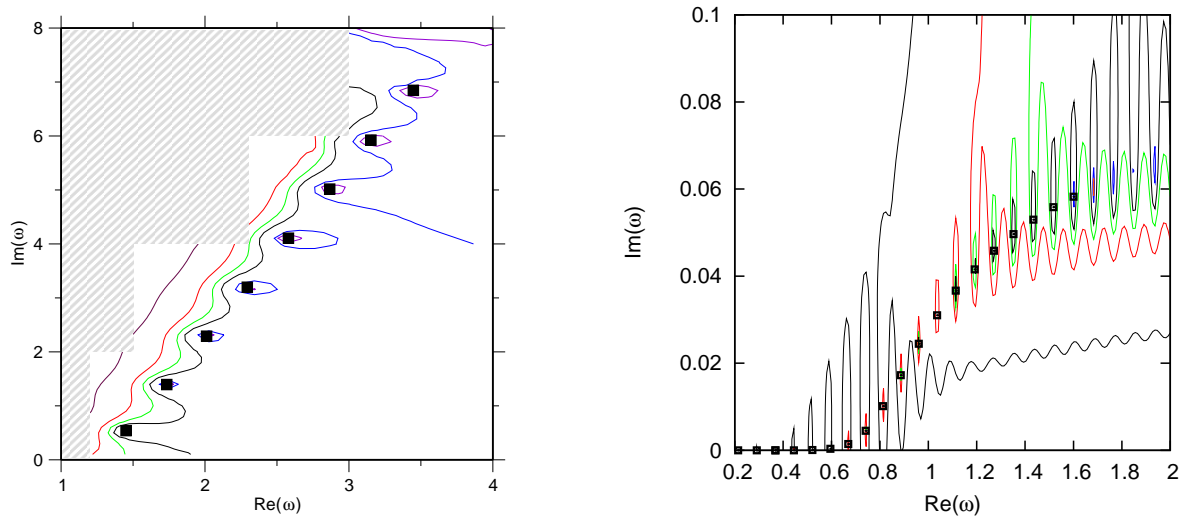


Figure 3: We plot the contours of $|g_s^{\text{tot}}(\tilde{\omega})|$, where $\tilde{\omega} = \omega\sqrt{R^3/3M}$. Quasi-normal modes correspond to zeros of this function and appear as “islands” in the plot. In the left panel we show the region in the complex $\tilde{\omega}$ -plane containing the interface modes. The shaded areas have not been covered due to convergence problems, mainly in the interior code, see main text for a discussion. Modes are displayed as black squares. The right panel shows the region containing the trapped modes and (a subset of) the curvature modes.

4 Conclusions

We have discussed a new approach to the quasinormal-mode problem in general relativity. By combining a characteristic formulation of the perturbation equations with the integration of a suitable phase-function for a complex valued radial coordinate, we have reformulated the standard outgoing-wave boundary condition as a zero Dirichlet condition. This brings a number of important advantages over previous strategies. The characteristic formulation permits coordinate compactification, which means that we can impose the boundary condition at future null infinity. The phase function avoids oscillatory behaviour in the solution, while the use of a complex radial variable allows a clean distinction between out- and ingoing waves. We have demonstrated that the method is straightforward to implement, and our analysis of two simple toy problems shows that it can lead to high precision numerical results. It is worth noting that the generalisation to unstable modes is straightforward, only requiring an alteration of the integration contour.

Even though the numerical results we have presented are in themselves of no great interest, the new method may represent a breakthrough in this area. Most importantly, we have every reason to believe that it should generalise to the problem of rapidly rotating relativistic stars. In that case one would no longer deal with a simple one-dimensional wave equation in the exterior vacuum. The lack of workable implementations of the required outgoing-wave conditions in that problem has been holding back progress for many years. Our new approach may be the key that unlocks this problem. Of course, we are still some steps away from implementing our new ideas for rotating star spacetimes. Most importantly, we need to consider how the different ingredients in our prescription generalise to this more complicated problem. This is an interesting challenge and we would hope to make progress on it in the near future.

Acknowledgements

LS gratefully acknowledge support by a Marie Curie Intra-European Fellowship, contract number MEIF-CT-2005-009366. This work was also supported by PPARC through grant numbers PPA/G/S/2002/00038 and PP/E001025/1. NA acknowledges support from PPARC via Senior Research Fellowship no PP/C505791/1.

Finally, we acknowledge support from the EU-network ILIAS providing opportunity for valuable discussions with our European colleagues.

A Constant density sphere – w -modes.

We test the code by computing the w -modes of a uniform sphere of mass $M \neq 0$. In the interior the background line element can be written

$$ds^2 = -e^{2\nu} dt^2 + e^{2\lambda} dr^2 + r^2(d\theta^2 + \sin^2 \theta d\phi) \quad (43)$$

where

$$e^\nu = \frac{1}{2} \left(3\sqrt{1 - \frac{2M}{R}} - \sqrt{1 - \frac{2Mr^2}{R^3}} \right) \quad (44)$$

$$e^{-\lambda} = \sqrt{1 - \frac{2Mr^2}{R^3}} \quad (45)$$

see *e.g.* [26]. The perturbation equations can be put in the form [24]

$$r \frac{d\mathcal{X}_1}{dr} = -(l+2)\mathcal{X}_1 - e^{\lambda-\nu+\nu_c} \mathcal{X}_2 \quad (46)$$

$$r \frac{d\mathcal{X}_2}{dr} = -e^{\lambda-\nu-\nu_c} [(l-1)(l+2)e^{2\nu} - \omega^2 r^2] \mathcal{X}_1 - (l-1)\mathcal{X}_2 \quad (47)$$

where

$$\mathcal{X}_1 = i\omega r^{-(l+1)} \psi \quad (48)$$

$$\mathcal{X}_2 = -e^{\nu_c-\nu} \omega^2 r^{-l} \varphi \quad (49)$$

and ν_c is the central value of ν . The function φ can in this context be viewed as auxiliary and defined by equation (46)

At the centre of the star the regular solution behave as

$$\mathcal{X}_1 = \hat{\mathcal{X}}_1 \left\{ 1 - \frac{e^{-2\nu_c} \omega^2 + (l+2) \frac{M}{R^3} (e^{-\nu_c} - 2l)}{2(2l+3)} r^2 + O(r^4) \right\} \quad (50)$$

$$\mathcal{X}_2 = \hat{\mathcal{X}}_1 \left\{ -(l+2) + \frac{(l+4)e^{2\nu_c} \omega^2 - (l+2)(l-1) \frac{M}{R^3} (e^{-\nu_c} + 2l + 6)}{2(2l+3)} r^2 + O(r^4) \right\} \quad (51)$$

where $\hat{\mathcal{X}}_1$ is an arbitrary constant.

References

- [1] S. Chandrasekhar, Physical Review Letters **24**, 611 (1970).
- [2] J. L. Friedman and B. F. Schutz, Astrophys. J. **222**, 281 (1978).
- [3] K. D. Kokkotas and B. G. Schmidt, Liv. Rev. Rel. **2**, 2 (1999), qr-qc/9909058.
- [4] N. Andersson, Royal Society of London Proceedings Series A **439**, 47 (1992).
- [5] N. Andersson, K. D. Kokkotas, and B. F. Schutz, Mon. Not. R. Ast. Soc. **274**, 1039 (1995), gr-qc/9503014.

- [6] E. Berti, F. White, A. Maniopolou, and M. Bruni, *Mon. Not. R. Ast. Soc.* **358**, 923 (2005).
- [7] N. Stergioulas and J. L. Friedman, *Astrophys. J.* **492**, 301 (1998), [gr-qc/9705056](#).
- [8] S. M. Morsink, N. Stergioulas, and S. R. Blattnig, *Astrophys. J.* **510**, 854 (1999), [gr-qc/9806008](#).
- [9] S. Yoshida and Y. Eriguchi, *Astrophys. J.* **515**, 414 (1999), [astro-ph/9807254](#).
- [10] A. Maniopolou, Ph.D. thesis, School of Mathematics, University of Southampton, 2005.
- [11] K. Glampedakis and N. Andersson, *Classical and Quantum Gravity* **20**, 3441 (2003), [gr-qc/0304030](#).
- [12] M. R. Dubal, R. A. d’Inverno, and J. A. Vickers, *Phys. Rev. D* **58**, 044019 (1998).
- [13] K.-E. Thylwe, *J. Phys. A* **38**, 10007 (2005).
- [14] S. Chandrasekhar and V. Ferrari, *Proc. Roy. Soc. Lond. A* **432**, 247 (1991).
- [15] K. D. Kokkotas, *Mon. Not. R. Ast. Soc.* **268**, 1015 (1994).
- [16] H. Bondi, M. G. J. van der Burg, and A. W. K. Metzner, *Royal Society of London Proceedings Series A* **269**, 21 (1962).
- [17] R. K. Sachs, *Royal Society of London Proceedings Series A* **270**, 103 (1962).
- [18] J. P. Boyd, *Chebyshev and Fourier Spectral Methods*, second revised ed. (Dover Publications, New York, USA, 2001).
- [19] S. Chandrasekhar and V. Ferrari, *Proc. Roy. Soc. Lond. A* **434**, 449 (1991).
- [20] N. Andersson, Y. Kojima, and K. D. Kokkotas, *Astrophys. J.* **462**, 855 (1996).
- [21] K. Tominaga, M. Saijo, and K.-I. Maeda, *Phys. Rev. D* **60**, 024004 (1999), [gr-qc/9901040](#).
- [22] K. D. Kokkotas and B. F. Schutz, *Mon. Not. R. Ast. Soc.* **255**, 119 (1992).
- [23] M. Leins, H.-P. Nollert, and M. H. Soffel, *Phys. Rev. D* **48**, 3467 (1993).
- [24] M. Karlovini and L. Samuelsson, *Class. Quantum Grav.* **24**, 3171 (2007), [gr-qc/0703001](#).
- [25] K. D. Kokkotas, *Mon. Not. R. Ast. Soc.* **277**, 1599 (1995).
- [26] B. F. Schutz, *A first course in general relativity* (Cambridge University Press, Cambridge, U.K., 1985).